



An assessment of the differences between spatial resolution and grid size for the SMAP enhanced soil moisture product over homogeneous sites

A. Colliander^{a,*}, T.J. Jackson^b, S.K. Chan^a, P. O'Neill^c, R. Bindlish^c, M.H. Cosh^b, T. Caldwell^d, J.P. Walker^e, A. Berg^f, H. McNairn^g, M. Thibeault^h, J. Martínez-Fernándezⁱ, K.H. Jensen^j, J. Asanuma^k, M.S. Seyfried^l, D.D. Bosch^m, P.J. Starksⁿ, C. Holifield Collins^o, J.H. Prueger^p, Z. Su^q, E. Lopez-Baeza^r, S.H. Yueh^a

^a Jet Propulsion Laboratory, California Institute of Technology, 4800 Oak Grove Drive, Pasadena, CA 91109, USA

^b USDA ARS Hydrology and Remote Sensing Laboratory, Beltsville, MD, USA

^c NASA Goddard Space Flight Center, Greenbelt, MD, USA

^d University of Texas at Austin, TX, USA

^e Monash University, Australia

^f University of Guelph, Canada

^g Agriculture and Agri-food Canada, Canada

^h Comisión Nacional de Actividades Espaciales (CONAE), Argentina

ⁱ Instituto Hispano Luso de Investigaciones Agrarias (CIALE), Universidad de Salamanca, Spain

^j University of Copenhagen, Denmark

^k University of Tsukuba, Tsukuba, Japan

^l USDA ARS Northwest Watershed Management Research, Boise, ID, USA

^m USDA ARS Southeast Watershed Research, Tifton, GA, USA

ⁿ USDA ARS Grazinglands Research Laboratory, El Reno, OK, USA

^o USDA ARS Southwest Watershed Research, Tucson, AZ, USA

^p USDA ARS National Laboratory for Agriculture and the Environment, Ames, IA, USA

^q University of Twente, The Netherlands

^r University of Valencia, Spain

ARTICLE INFO

Keywords:

SMAP

Soil moisture

Spatial resolution

In situ

ABSTRACT

Satellite-based passive microwave remote sensing typically involves a scanning antenna that makes measurements at irregularly spaced locations. These locations can change on a day to day basis. Soil moisture products derived from satellite-based passive microwave remote sensing are usually resampled to a fixed Earth grid that facilitates their use in applications. In many cases the grid size is finer than the actual spatial resolution of the observation, and often this difference is not well understood by the user. Here, this issue was examined for the Soil Moisture Active Passive (SMAP) enhanced version of the passive-based soil moisture product, which has a grid size of 9-km and a nominal spatial resolution of 33-km. *In situ* observations from core validation sites were used to compute comparison metrics. For sites that satisfied the established reliability and scaling criteria, the impact of validating the 9-km grid product with *in situ* data collected over a 9-km versus a 33-km domain was very small for the sites studied (0.039 m³/m³ unbiased root mean square difference for the 9-km case versus 0.037 m³/m³ for the 33-km case). This result does not mean that the resolution of the product is 9-km but that for the conditions studied here the soil moisture estimated from *in situ* observations over 9-km is a close approximation of the soil moisture estimated from *in situ* observations over the 33-km resolution. The implication is that using the enhanced SMAP product at its grid resolution of 9-km should not introduce large errors in most applications.

1. Introduction

Most surface soil moisture remote sensing products based on passive

microwave radiometry involve observations that have spatial resolutions (defined as the 3 dB beamwidth, which is also referred to as the footprint) of 30 km or greater. In the process of providing users with

* Corresponding author.

E-mail address: andreas.colliander@jpl.nasa.gov (A. Colliander).

standardized products that facilitate applications, data assimilation and modeling, the observations are usually resampled to a fixed Earth grid. In the context of this paper, the spatial resolution is defined as the spatial domain that contributes to the 3 dB footprint of the sensor and grid size is the spatial interval used in the sampling of the sensor measurements. The above is true for the Soil Moisture Active Passive (SMAP) (Chan et al., 2018), Soil Moisture Ocean Salinity (SMOS) (SMOS L3 Product at Centre Aval de Traitement des Données SMOS (CATDS), 2016), and Advanced Microwave Scanning Radiometer 2 (AMSR2) missions (Descriptions of GCOM-W1 AMSR2 Level 1R and Level 2 Algorithms, 2013). In the case of SMAP, which is the focus of this paper, the standard radiometer-based product (L2SMP) has a grid size of 36-km, which is close to the nominal spatial resolution of the sensor (Chan et al., 2016a). In such cases, the terms spatial resolution and grid size have been used interchangeably.

All of the missions noted above now provide products that have been resampled to grid sizes (9 to 25 km) that are significantly finer than the nominal spatial resolutions of the sensor. The actual spatial domain that these grid products represent may not be clear to the user.

For SMAP, there is considerable overlap of footprints across a scan. This is exploited through an interpolation approach to create an enhanced SMAP brightness temperature (TB) product with a grid size of 9-km that is the basis for the 9-km enhanced soil moisture product (L2SMP_E) with a grid size of 9-km (Chan et al., 2018). Although it is stated in supporting documents that the actual contributing domain is larger than 9-km, the reality is that many users will utilize the data as if its spatial resolution was the same as the grid size. When interpreted in this manner, the user implicitly assumes that the actual soil moisture for the 9-km grid cell domain is not much different than the retrieval value, which is based on a TB and ancillary data for the nominal spatial resolution (the nominal spatial resolution specified for the L2SMP_E is 33-km; a full description of this will be provided in a following section). It is reasonable to think that soil moisture at 9-km and 33-km would be correlated; however, it should be recognized that meteorological variability and geophysical heterogeneity over the domains may influence this relationship.

In this investigation we examine the magnitude of the difference between soil moisture estimates made using *in situ* observations over 9 and 33-km domains and also compare these to L2SMP_E retrievals to assess the likely impact of assuming that grid size equals spatial resolution. Analyses presented in this study are based on satellite and *in situ* soil moisture data collected over the SMAP core validation sites (CVS) (Colliander et al., 2017). While there have been no systematic studies that have directly addressed this issue for remotely sensed soil moisture, Dumedah et al. (2014) assessed the SMOS brightness temperature products that were resampled from a 42 km spatial resolution to a 15 km grid size using high resolution aircraft measurements and found that the differences could be < 4 K in some cases, which corresponds to only about $0.01 \text{ m}^3/\text{m}^3$ soil moisture over bare surfaces at horizontal polarization (e.g., Njoku and Entekhabi, 1996).

2. Data

2.1. The SMAP level 2 soil moisture passive enhanced (L2SMP_E) product

The L2SMP_E is made possible by an enhanced interpolation of the SMAP Level 1B Brightness Temperature Product (L1BTB) (Chaubell et al., 2016; Peng et al., 2017). The approach is based on the Backus-Gilbert (BG) optimal interpolation technique (Poe, 1990) applied to the original standard TB data, where the objective of the BG interpolation, as implemented by SMAP, is to achieve optimal data estimates at unsampled locations as if observations were actually made with the original sensor at those same locations. This interpolation provides an improvement over the standard SMAP Level 1C Gridded Brightness Temperature Product (L1CTB) (Chan et al., 2016b; Piepmeier et al., 2017; Peng et al., 2017), in that it makes explicit use of antenna pattern

information and finer grid size to more fully capture the information of the oversampled radiometer measurements in the along-scan direction. It is important to note that this recovery of high frequency sampling information as implemented in the BG approach comes primarily from interpolation rather than resolution enhancement. Thus, the native resolution of the interpolated data remains similar to the spatial extent covered by the 3 dB beamwidth of the radiometer (~ 40 km). The resulting interpolated data, known as the SMAP Enhanced Level 1 Gridded Brightness Temperature Product (L1CTB_E), are provided on the 9-km EASE Grid 2.0 projection. The product is used as the primary input to subsequent geophysical inversion to produce the SMAP L2SMP_E. The soil moisture algorithm, the Single Channel Algorithm-V Polarization (SCA-V), is the same as that used in the standard product (O'Neill et al., 2016); several alternative algorithms were included in the assessments in previous reports (Chan et al., 2016a, 2018). Since these comparisons have consistently shown that the SCA-V has the best performance metrics, this study only examines the SCA-V.

Because after BG interpolation the native resolution of the L1CTB_E remains approximately the same as the 3 dB spatial resolution of the SMAP radiometer, as noted above, it is important in the subsequent soil moisture inversion process that a proper contributing domain is chosen to accurately reflect the actual spatial extent observed by the radiometer. The relationship between grid size and contributing domain is illustrated in Fig. 1 using a typical core validation site. As described in Chan et al. (2018), in order to facilitate processing (considering the resolution of ancillary data and the structure of the EASE grid) a contributing domain of 33-km was chosen to approximate the spatial extent covered by the radiometer (spatial resolution). Chan et al. (2018) noted that a change in contributing domain from 36-km to 33-km had almost no impact on the validation metrics.

2.2. Core validation sites

The primary validation for the L2SMP_E soil moisture product is based on a comparison of SMAP retrievals with ground-based observations that have been verified as being capable of providing an estimate of the soil moisture over the same spatial domain (33-km) and depth (5 cm). The locations that provide these validation observations are called CVS (Colliander et al., 2017). The validation comparisons provide error estimates and a basis for modifying algorithms and/or

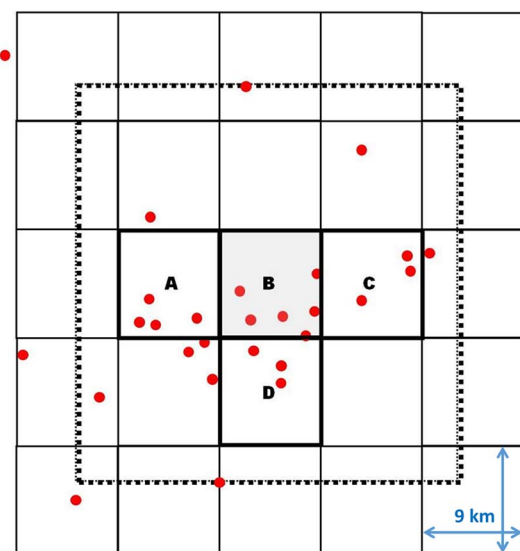


Fig. 1. Example of the SMAP L2SMP_E grid over a core validation site (Walnut Gulch). The solid black lines indicate the borders of the 9-km grid cells. The circles are the locations of *in situ* stations. The CVS 9-km grid cell is chosen (the heavier black line grid cell “B”) so that its actual contributing domain of 33-km (the dashed black line centered on grid cell “B”) best captures the data from the local network of stations.

Table 1

Core validation site names, location, climate regime, and the dominant International Geosphere-Biosphere Programme (IGBP) land cover type for SMAP. The number of grids at a size of 33 and 9-km within each site are also listed.

| | Site name | Number of grids cells | | | Area | Climate regime | Dominant land cover |
|----|----------------|----------------------------|--------------|-----------------|----------------|----------------|---------------------|
| | | L2SMP_E 33-km ^a | L2SMP_E 9-km | L2SMP_E Matched | | | |
| 1 | Walnut Gulch | 1 | 4 | 4 | USA (Arizona) | Arid | Shrub open |
| 2 | Reynolds Creek | 1 | 1 | | USA (Idaho) | Arid | Grasslands |
| 3 | Fort Cobb | 1 | 1 | 1 | USA (Oklahoma) | Temperate | Grasslands |
| 4 | Little Washita | 1 | 1 | | USA (Oklahoma) | Temperate | Grasslands |
| 5 | South Fork | 1 | 1 | 1 | USA (Iowa) | Cold | Croplands |
| 6 | Little River | 1 | 1 | | USA (Georgia) | Temperate | Crop/natural mosaic |
| 7 | TxSON | 1 | 2 | 2 | USA (Texas) | Temperate | Grasslands |
| 8 | Kenaston | 1 | 3 | 1 | Canada | Cold | Croplands |
| 9 | Carman | 1 | 1 | | Canada | Cold | Croplands |
| 10 | Monte Buey | 1 | 1 | | Argentina | Temperate | Croplands |
| 11 | REMEDHUS | 1 | 1 | | Spain | Temperate | Croplands |
| 12 | Valencia | | 1 | | Spain | Arid | Woody Savannas |
| 13 | Twente | 1 | | | Netherlands | Temperate | Crop/natural mosaic |
| 14 | HOBE | 1 | 1 | 1 | Denmark | Temperate | Croplands |
| 15 | Mongolia | 1 | | | Mongolia | Cold | Grasslands |
| 16 | Yanco | 1 | 2 | 2 | Australia | Arid | Croplands |

^a Included in the Chan et al. (2018) analysis.

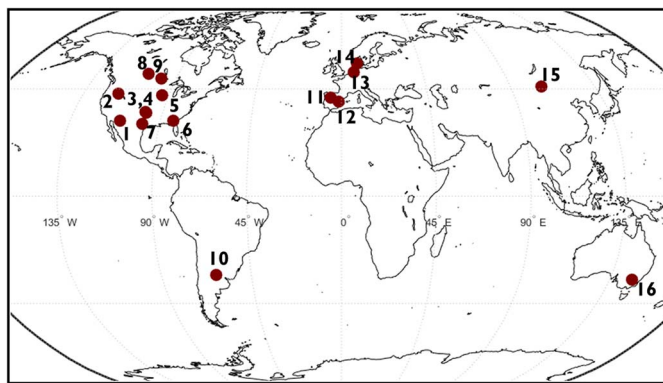


Fig. 2. Locations of the core validation sites (CVS) used in the study.

parameters. Table 1 summarizes those CVS used in the current study and Fig. 2 shows their respective geographic locations. One of the criteria used for selecting a local set of stations (network) as a CVS in the L2SMP_E validation (Chan et al., 2018) was that it included at least 9 stations distributed over the contributing domain (33-km). This decision was based upon published studies of soil moisture variability at different scales (Famiglietti et al., 2008). A similar analysis indicated that if the domain was 9-km, 5 stations would be required to meet the same criteria (Colliander et al., 2017). Furthermore, Table 2 shows the land cover fractions for the 33-km and 9-km pixels at the sites. If a site included more than one pixel at a scale the range of land cover fractions is given. The values show that the pixels at the two different scales share similar land cover decomposition which means the land cover decompositions of the sites are generally homogeneous across the scales.

Table 2

Land cover fractions for the 33-km and 9-km pixels based on the IGBP classification. The columns include the range of land cover fractions when multiple pixels within the site are used.

| | Site name | Land cover fractions for 33-km pixels | | | | | Land cover fractions for 9-km pixels | | | | |
|----|-----------------------------|---------------------------------------|------------------|--------------------|--------------------|--------------------|--------------------------------------|------------------|--------------------|--------------------|--------------------|
| | | Gr. ^a | Cr. ^b | Cr/M. ^c | Sh/O. ^d | Sa/W. ^e | Gr. ^a | Cr. ^b | Cr/M. ^c | Sh/O. ^d | Sa/W. ^e |
| 1 | Walnut Gulch | 33–38% | | | 62–67% | | 32–68% | | | 32–68% | |
| 2 | Reynolds Creek ^f | 95% | 1% | | | | 85% | | | | |
| 3 | Fort Cobb | 91–94% | 5–8% | | | | 100% | | | | |
| 4 | Little Washita | 98% | 1% | | | | 98% | 1% | | | 1% |
| 5 | South Fork | | 100% | | | | | 100% | | | |
| 6 | Little River ^g | | 20% | 57% | | 15% | | 4% | 62% | | 20% |
| 7 | TxSON ^h | 83–92% | 0–1% | | | 2–7% | 65–98% | | | | 0–8% |
| 8 | Kenaston | 1% | 99% | | | | 0–1% | 99–100% | | | |
| 9 | Carman | | 100% | | | | | 100% | | | |
| 10 | Monte Buey | | 100% | | | | | 100% | | | |
| 11 | REMEDHUS | | 83% | | 17% | | | 86% | | 14% | |
| 12 | Valencia | – | – | – | – | – | | 46% | | 6% | 48% |
| 13 | Twente ^g | 2% | 9% | 67% | | | – | – | – | – | – |
| 14 | HOBE ^g | 1% | 65% | 16% | | | 1% | 49% | 11% | | |
| 15 | Mongolia | 100% | | | | | – | – | – | – | – |
| 16 | Yanco | 43–63% | 27–39% | | 9–16% | 1–9% | 56–83% | 5–35% | | 10–12% | |

^a Grasslands.

^b Croplands.

^c Croplands/natural mosaic.

^d Shrub open.

^e Savannas woody.

^f Part of Reynolds Creek is covered by the Forest Evergreen Needle Leaf class.

^g Part of Little River, Twente and HOBE is covered by the Forest Mixed class.

^h Part of TxSON is covered by the Savanna class.

Three sets of data from the CVS sites will be utilized here. The first is that described above that consists of the single most representative 9-km grid cell location (defined as that with the best density (minimum of 9) and distribution of stations within the 33-km contributing domain centered on that grid cell). These sites are indicated in Column 3 of Table 1. In the example shown in Fig. 1, this would be the grid cell marked “B”. The important characteristic of this data set is that they were selected to satisfy the validation criteria for a 33-km domain.

The second data set that will be utilized consists of all 9-km grid cells within the CVS that had at least 5 ground stations. The number at each CVS is listed in Table 1 Column 4. Referring to the example in Fig. 1, A, B, C, and D all would meet the criteria.

Finally, the third data set consists of all 9-km grid cells that satisfy the criteria of both the 33 and 9-km validation described above; at least 9 stations over the 33-km domain and at least 5 over the 9-km domain. This will be referred to as the matched data set. For the Fig. 1 example, the criteria are met at both scales for the four grid cells (A, B, C, and D). Column 5 of Table 1 gives the number of grid cells at the CVS location that satisfy the criteria for both scales.

3. Methods

All available *in situ* and SMAP retrievals between April 1, 2015 and April 1, 2017 were used in the analyses presented here. Coverage is typically every 2–3 days. As noted above, only the SCA-V results are presented because this is the algorithm found to work best with SMAP. In addition, the discussion will focus on the descending (am) retrievals because the metrics of the ascending (pm) retrievals have been found to be similar to those of the descending retrievals (Chan et al., 2018).

Considering the data that are available, one way to assess the impact of the grid size *versus* product resolution is to compare soil moisture estimates over the collocated 9-km and 33-km domains derived from *in situ* observations (identified in Column 5 of Table 1). There are at least three limitations in conducting such an analysis. First, a robust analysis requires long periods of record for many meteorological and geophysical conditions, here we are restricted to the CVS available and the period of record of SMAP. Second, the quality of the soil moisture estimates based on the *in situ* observations will be dependent on the quality of the measurements and the sample size (number of stations used to compute the average). Therefore, even if *in situ*-based soil moisture estimates exist for collocated 9-km and 33-km grids, there will be uncertainty associated with each estimate of the average. Finally, data points used to compute the 9-km averages are also used in the 33-km averages. The last column in Table 3 shows the fraction of 33-km stations that are used to compute the 9-km average. In some instances, the percentage is high (TxSON, Yanco), but in these cases there is a cluster of stations within the 9-km grid cell, so the percentage does not represent spatial overlap of stations. Furthermore, the average soil moistures are estimated through an up-scaling function which in most cases for 33-km involves spatial weighting, which prevents the clusters from over-representing in the estimated average.

Another approach to assessing the impact of the grid size/spatial resolution issue is to consider how it affects the validation metrics of SMAP. This is achieved through a comparison of SMAP retrievals to *in situ*. This approach increases the number of CVS that can be used, thus making the analysis more robust. In this analysis, the metrics obtained with the original 33-km scale validation approach are compared with the metrics obtained with the 9-km *in situ* grids. All available 9-km grid cells as well as the matched data set are used as described in Section 2.2.

In the comparative analysis presented below four metrics were computed: root mean square difference (RMSD), unbiased RMSD (ubRMSD), Pearson correlation (R) and bias. The ubRMSD is defined as follows:

Table 3

Differences in average *in situ* soil moisture for matched 9- and 33-km grids for the time period between April 1, 2015 and April 1, 2017 (33-km minus 9-km). Metrics shown are the unbiased root mean square difference (ubRMSD), bias, the root mean square difference (RMSD), and the Pearson correlation coefficient (R) between the two scales. The number of samples (N) evaluated and the size of the 9-km station subset as the percentage of the 33-km stations are also given.

| Site name | ubRMSD (m ³ /m ³) | Bias (m ³ /m ³) | RMSD (m ³ /m ³) | R | N | % of 9-km stations |
|------------------------|--|--|--|--------------|--------|--------------------|
| Walnut | 0.014 | 0.002 | 0.019 | 0.917 | | |
| <i>Gulch</i> | | | | | | |
| Walnut | 0.010 | 0.005 | 0.012 | 0.923 | 20,003 | 28% |
| <i>Gulch-A</i> | | | | | | |
| Walnut | 0.017 | −0.012 | 0.021 | 0.896 | 15,176 | 20% |
| <i>Gulch-B</i> | | | | | | |
| Walnut | 0.016 | 0.022 | 0.027 | 0.889 | 17,155 | 19% |
| <i>Gulch-C</i> | | | | | | |
| Walnut | 0.011 | −0.008 | 0.014 | 0.958 | 23,049 | 18% |
| <i>Gulch-D</i> | | | | | | |
| TxSON | 0.014 | 0.012 | 0.018 | 0.980 | | |
| <i>TxSON-A</i> | 0.012 | 0.009 | 0.015 | 0.986 | 15,497 | 71% |
| <i>TxSON-B</i> | 0.015 | 0.014 | 0.020 | 0.974 | 14,255 | 56% |
| Fort Cobb | 0.015 | 0.010 | 0.018 | 0.968 | 29,019 | 31% |
| South Fork | 0.018 | −0.017 | 0.025 | 0.960 | 10,641 | 21% |
| Kenaston | 0.022 | −0.039 | 0.045 | 0.896 | 6290 | 17% |
| HOBE | 0.012 | 0.000 | 0.012 | 0.976 | 4614 | 40% |
| Yanco | 0.031 | −0.029 | 0.042 | 0.955 | | |
| <i>Yanco-A</i> | 0.019 | −0.021 | 0.028 | 0.983 | 34,525 | 60% |
| <i>Yanco-B</i> | 0.042 | −0.036 | 0.055 | 0.927 | 38,005 | 31% |
| Overall results | 0.018 | −0.009 | 0.025 | 0.950 | | |

$$ubRMSD = \sqrt{\frac{\sum_{i=1}^N ((x_i - \bar{x}) - (y_i - \bar{y}))^2}{N - 1}}$$

where *N* is the number of samples in datasets *x* and *y* (the equation of ubRMSD is equivalent to standard deviation of the difference of *x* and *y*). Note that in the text below, the terms RMSE (root mean square error) and ubRMSE are used also. They are computed similarly as RMSD and ubRMSD but are used when referring to *in situ vs.* SMAP product comparisons (rather than *in situ vs. in situ* comparisons) in order to differentiate the nature of these comparisons.

4. Results

Table 3 summarizes the results of the matched *in situ* data set inter-comparisons described in Section 3. As shown in Table 1 Column 5 there is a total of 12 grid locations that satisfy both criteria. In order to not bias the results to a particular locale, the metrics for CVS with multiple grid cells were averaged, resulting in 7 values that were then averaged to compute the overall results. For instance, the four individual 9-km grid cells in Walnut Gulch shown in italics in Table 3 were averaged to compute the Walnut Gulch average metrics indicated in bold. The results exhibit some variability in bias between sites but have an overall bias near zero. The ubRMSD was more consistent among the individual grid cells with a value < 0.02 m³/m³. The R was very high (0.95). Based upon this limited but diverse set of sites, if a user of the L2SMP_E product was to assume that the soil moisture averages over 9-km and 33-km domains are similar, it is not likely to introduce significant error into an application.

The L2SMP_E CVS summary results based upon using the CVS that meet the criteria (at least 9 stations over a 33-km domain) are presented at the bottom of Table 4 as the row labeled L2SMP_E 33-km All Sites. This is the same as the analyses presented in Chan et al. (2018) except it is updated through April 1, 2017. Various aspects of the performance of the algorithm at the sites were presented in Chan et al. (2018); the most relevant being that the product meets the SMAP mission performance criteria (ubRMSE < 0.04 m³/m³) with low bias (it is noted that this is

Table 4

Performance metrics (unbiased root mean square error, ubRMSE; bias, and root mean square error, RMSE) of the L2SMP_E product (SCA-V algorithm) for the AM overpasses over 9-km reference pixels for the time period between April 1, 2015 and April 1, 2017. The correlation coefficient (R) and the number of samples (N) are also shown.

| Site name | ubRMSE (m ³ /m ³) | Bias (m ³ /m ³) | RMSE (m ³ /m ³) | R | N | Latitude (degrees) | Longitude (degrees) |
|--------------------------------|--|--|--|--------------|------------|--------------------|---------------------|
| Reynolds Creek | 0.039 | -0.047 | 0.061 | 0.733 | 46 | 43.0916 | -116.748 |
| Walnut Gulch* | 0.025 | 0.004 | 0.027 | 0.782 | | | |
| <i>Walnut Gulch-A</i> | <i>0.024</i> | <i>0.009</i> | <i>0.026</i> | <i>0.816</i> | <i>157</i> | <i>31.7488</i> | <i>-110.026</i> |
| <i>Walnut Gulch-B</i> | <i>0.030</i> | <i>-0.009</i> | <i>0.031</i> | <i>0.676</i> | <i>188</i> | <i>31.7488</i> | <i>-110.119</i> |
| <i>Walnut Gulch-C</i> | <i>0.024</i> | <i>0.012</i> | <i>0.027</i> | <i>0.808</i> | <i>127</i> | <i>31.6661</i> | <i>-110.026</i> |
| <i>Walnut Gulch-D</i> | <i>0.022</i> | <i>0.004</i> | <i>0.022</i> | <i>0.827</i> | <i>175</i> | <i>31.7488</i> | <i>-109.933</i> |
| TxSON* | 0.028 | 0.001 | 0.028 | 0.940 | | | |
| <i>TxSON-A</i> | <i>0.025</i> | <i>0.003</i> | <i>0.025</i> | <i>0.932</i> | <i>306</i> | <i>30.4342</i> | <i>-98.8226</i> |
| <i>TxSON-B</i> | <i>0.031</i> | <i>-0.002</i> | <i>0.031</i> | <i>0.947</i> | <i>237</i> | <i>30.2711</i> | <i>-98.7293</i> |
| Fort Cobb* | 0.024 | -0.042 | 0.048 | 0.911 | 288 | 35.3783 | -98.5425 |
| Little Washita | 0.027 | 0.004 | 0.027 | 0.858 | 224 | 34.9483 | -98.0757 |
| South Fork* | 0.053 | -0.074 | 0.091 | 0.631 | 203 | 42.4225 | -93.4077 |
| Little River | 0.030 | 0.107 | 0.111 | 0.845 | 141 | 31.7488 | -83.6981 |
| Kenaston | 0.030 | -0.052 | 0.061 | 0.786 | | | |
| <i>Kenaston-A</i> | <i>0.031</i> | <i>-0.035</i> | <i>0.047</i> | <i>0.749</i> | <i>167</i> | <i>51.3569</i> | <i>-106.478</i> |
| <i>Kenaston-B*</i> | <i>0.028</i> | <i>-0.078</i> | <i>0.083</i> | <i>0.833</i> | <i>157</i> | <i>51.4691</i> | <i>-106.478</i> |
| <i>Kenaston-C</i> | <i>0.031</i> | <i>-0.043</i> | <i>0.053</i> | <i>0.775</i> | <i>148</i> | <i>51.3569</i> | <i>-106.385</i> |
| Carman | 0.066 | -0.073 | 0.098 | 0.446 | 141 | 49.7038 | -97.9824 |
| Monte Buey | 0.062 | -0.029 | 0.068 | 0.883 | 128 | -32.9981 | -62.5052 |
| REMEDHUS | 0.039 | -0.001 | 0.039 | 0.864 | 312 | 41.2916 | -5.555 |
| Valencia | 0.032 | -0.005 | 0.033 | 0.576 | 94 | 39.5394 | -1.2604 |
| HOBE* | 0.034 | -0.008 | 0.035 | 0.686 | 64 | 55.9652 | 9.1027 |
| Yanco* | 0.050 | 0.000 | 0.051 | 0.918 | | | |
| <i>Yanco-A</i> | <i>0.054</i> | <i>-0.011</i> | <i>0.056</i> | <i>0.881</i> | <i>252</i> | <i>-34.6914</i> | <i>146.0633</i> |
| <i>Yanco-B</i> | <i>0.045</i> | <i>0.011</i> | <i>0.046</i> | <i>0.955</i> | <i>250</i> | <i>-34.9483</i> | <i>146.3434</i> |
| L2SMP_E 9-km All Sites | 0.038 | -0.013 | 0.055 | 0.779 | | | |
| L2SMP_E 33-km All Sites | 0.038 | -0.013 | 0.053 | 0.805 | | | |
| *L2SMP_E Matched 33-km | 0.035 | -0.028 | 0.052 | 0.814 | | | |
| *L2SMP_E Matched 9-km | 0.035 | -0.019 | 0.049 | 0.836 | | | |

Italics: one of the multiple pixels at the site. Bold: site result (average if multiple pixels at the site). Bold Italics: Mean value.

the average result; 0.04 m³/m³ criterion is not met with every site). This establishes the accuracy expected when using the SMAP L2SMP_E product at a 33-km spatial resolution.

Next, the validation metrics (retrieval vs. *in situ*) were computed using all 9-km CVS grids with at least five *in situ* sites (Column 3 in Table 1). These results are reported in Table 4. In some cases, there were multiple 9-km CVS at a location and in others, no 9-km box was viable (*i.e.*, Twente and Mongolia). As noted above, in order not to bias the results to a particular network, the values for each location with multiple grid cells (*i.e.* Walnut Gulch) were first averaged. These averages were then combined with the sites having only a single 9-km CVS to determine the overall averages for the metrics. At the bottom of

Table 4, the summary for the 33-km analyses can be compared to the 9-km validation results (L2SMP_E 9-km All Sites). The mean ubRMSE and bias are identical with a small decrease in correlation, which is expected because when comparing to the 9-km we are ignoring the variability that may occur outside this domain. Fig. 3 shows the distribution of the difference between metrics obtained with 33-km grid cells and 9-km grid cells at each CVS. Only the CVS with both 33-km and 9-km pixels were included. The resulting distributions do not clearly follow a normal distribution although they are not contrary to it either (the small sample size does not allow a robust use of statistical methods for making this determination), and the median differences and the distribution of the values do not reveal any skew in the results

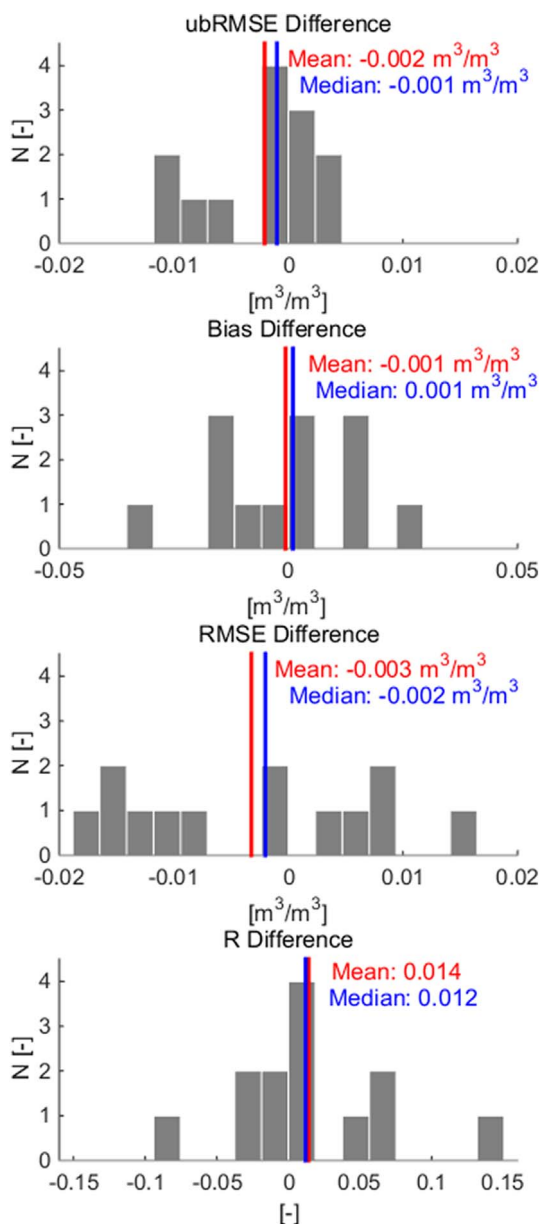


Fig. 3. Distribution of the differences between metrics obtained with 33-km grid cells and 9-km grid cells (33-km minus 9-km).

either. These results support the conclusion that, for the range of conditions examined here for generally homogeneous sites, very little error was introduced by assuming that the spatial resolution equals the 9-km grid size.

A final assessment was conducted using only the sites at which collocated 33-km and 9-km CVS could be identified. These results are presented on the last two rows of Table 4 and support the conclusion reached previously.

5. Conclusion

Recognizing that it is common practice for users to apply passive microwave-based soil moisture products provided at a particular grid size (here 9-km for SMAP) as an estimate of the soil moisture for that grid rather than the nominal contributing domain (here 33-km) it represents, the impact of this assumption was assessed for SMAP L2SMP_E products. For the sites that satisfied the established CVS criteria, the difference in the average soil moisture over collocated 9-km and 33-km

was very small. In addition, the impact of this assumption on validation metrics was also very small. These results do not mean that the resolution of the product is 9-km but, rather, that for the conditions studied that include generally homogeneous sites, the soil moisture interpolated at the 9-km grid size is a good approximation of the soil moisture measured over satellite's 33-km resolution. Naturally there are situations where the soil moisture for a 9-km area can be significantly different from the surrounding larger domain, and in applications focusing on a single pixel or very localized conditions the impact of the small-scale heterogeneity must be determined separately. Also, in case of spatial downscaling the 33-km domain is the appropriate scale to start from because this is the scale the product actually represents. However, for applications operating on larger domains (not dominated by single pixels) the result implies that using the SMAP enhanced product at its interpolated 9-km grid size would not introduce large errors.

Acknowledgements

We would like to thank the four anonymous reviewers and the Remote Sensing of Environment editorial team whose efforts helped to improve this manuscript. The research described in this publication was carried out at in part the Jet Propulsion Laboratory, California Institute of Technology, under a contract with the National Aeronautics and Space Administration. The University of Salamanca team involvement in this study was supported by the Spanish Ministry of Economy and Competitiveness with the projects ESP2015-67549-C3 and ESP2017-89463-C3-3-R, and the European Regional Development Fund (ERDF).

References

- Chan, S., Bindlish, R., O'Neill, P., Njoku, E., Jackson, T.J., Colliander, A., Chen, F., Burgin, M., Dunbar, R.S., Piepmeier, J., Yueh, S., Entekhabi, D., Cosh, M.H., Seyfried, M.S., Bosch, D.D., Starks, P., Goodrich, D.C., Prueger, J.H., Crow, W.T., Caldwell, T., Walker, J., Wu, X., Pacheco, A., McNairn, H., Anderson, M.C., 2016a. Assessment of the SMAP Level 2 passive soil moisture product. *IEEE Trans. Geosci. Remote Sens.* 54 (8), 4994–5007.
- Chan, S., Njoku, E.G., Colliander, A., 2016b. SMAP L1C Radiometer Half-orbit 36 km EASE-grid Brightness Temperatures, Version 3. NASA National Snow and Ice Data Center Distributed Active Archive Center, Boulder, Colorado USA. <http://dx.doi.org/10.5067/E51BSP6V3KP7>.
- Chan, S., Bindlish, R., O'Neill, P.E., Jackson, T.J., Njoku, E., Dunbar, R.S., Chaubell, J., Piepmeier, J., Yueh, S., Entekhabi, D., Colliander, A., Chen, F., Cosh, M.H., Caldwell, T., Walker, J., Berg, A., McNairn, H., Thibeault, M., Martinez-Fernandez, J., Udall, F., Seyfried, M.S., Bosch, D.D., Starks, P., Holyfield Collins, C., Prueger, J.H., 2018. Development and assessment of the SMAP enhanced passive soil moisture product. *Remote Sens. Environ.* 204, 931–941.
- Chaubell, M.J., Chan, S., Dunbar, R.S., Peng, J., Yueh, S., 2016. SMAP Enhanced L1C Radiometer Half-orbit 9-km EASE-grid Brightness Temperatures, Version 1. 2016 NASA National Snow and Ice Data Center Distributed Active Archive Center, Boulder, Colorado USA. <http://dx.doi.org/10.5067/2C909KT6JAWS>.
- Colliander, A., Jackson, T.J., Bindlish, R., Chan, S., et al., 2017. Validation of SMAP surface soil moisture products with core validation sites. *Remote Sens. Environ.* 191, 215–231.
- Descriptions of GCOM-W1 AMSR2 Level 1R and Level 2 Algorithms. [online] Available: http://suzaku.eorc.jaxa.jp/GCOM_W/data/doc/NDX-120015A.pdf.
- Dumedah, G., Walker, J.P., Rüdiger, C., 2014. Can SMOS data be used directly on the 15-km discrete global grid? *IEEE Trans. Geosci. Remote Sens.* 52 (5), 2538–2544.
- Famiglietti, J.S., Ryu, D., Berg, A., Rodell, M., Jackson, T.J., 2008. Field observations of soil moisture variability across scales. *Water Resour. Res.* 44, W01423. <http://dx.doi.org/10.1029/2006WR005804>.
- Njoku, E., Entekhabi, D., Oct. 1996. Passive microwave remote sensing of soil moisture. *J. Hydrol.* 184 (1/2), 101–129.
- O'Neill, P.E., Chan, S., Njoku, E.G., Jackson, T., Bindlish, R., 2016. SMAP Enhanced L2 Radiometer Half-orbit 9-km EASE-grid Soil Moisture, Version 1. 2016 NASA National Snow and Ice Data Center Distributed Active Archive Center, Boulder, CO. <http://dx.doi.org/10.5067/CE0K6JS5WQMM>.
- Peng, J., Misra, S., Piepmeier, J.R., Dinnat, E.P., Hudson, D., Le Vine, D.M., De Amici, G., Mohammed, P.N., Bindlish, R., Yueh, S.H., Meissner, T., Jackson, T.J., 2017. Soil moisture active/passive (SMAP) L-band microwave radiometer post-launch calibration. *IEEE Trans. Geosci. Remote Sens.* 55 (4), 1897–1914.
- Piepmeier, J.R., Focardi, P., Horgan, K.A., Knuble, J., Ehsan, N., Lucey, J., Brambor, C., Brown, P.R., et al., 2017. SMAP L-band microwave radiometer: instrument design and first year on orbit. *IEEE Trans. Geosci. Remote Sens.* 55 (4), 1954–1966.
- Poe, G., 1990. Optimum interpolation of imaging microwave radiometer data. *IEEE Trans. Geosci. Remote Sens.* 28 (5), 800–810.
- SMOS L3 Product at Centre Aval de Traitement des Données SMOS (CATDS). [online] Available: <http://www.catds.fr/Products/Available-products-from-CPDC>.